J|A|C|S COMMUNICATIONS

Published on Web 07/01/2010

Modifying the Size and Shape of Monodisperse Bifunctional Alkaline-Earth Fluoride Nanocrystals through Lanthanide Doping

Daqin Chen, Yunlong Yu, Feng Huang, Ping Huang, Anping Yang, and Yuansheng Wang*

State Key Laboratory of Structural Chemistry, Fujian Institute of Research on the Structure of Matter, Chinese Academy of Sciences, Fuzhou, Fujian 350002, P. R. China

Received April 29, 2010; E-mail: yswang@fjirsm.ac.cn

Abstract: In this communication, a simple route for modifying the uneven size and shape of alkaline-earth fluoride nanophases to monodisperse ultrasmall nanospheres through lanthanide doping is offered. These nanospheres are found to exhibit bifunctionality, i.e., tunable upconversion emissions as well as proper paramagnetism, making them potentially applicable in the biological field. The synthesis strategy, which involves doping of an impurity with a different valence than the cation in the nanophase, might be useful for controlling the solution growth of some technologically important nanomaterials.

It is well-known that impurity doping is an important route for imparting new and useful properties for many functional nanomaterials. At present, great endeavors have been devoted to investigating the impact of nanocrystalline size and shape on the behaviors of dopants.[1−6] Conversely, impurity doping was recently found to have a significant influence on the growth of some functional nanomaterials as well. Wang and co-workers[7] reported the conversion of CeO_2 nanopolyhedra into nanospheres by Ti^{4+} doping, and Liu and co-workers[8] demonstrated rational tunability of the size and phase of $NaYF_4$ nanocrystals by lanthanide doping. However, there have been few systematic studies focusing on this subject to date, so it remains a large space worthy of exploration.

This communication reports that using trivalent lanthanide (Ln^{3+}) ions to substitute for divalent strontium ions in SrF_2 nanocrystals allows products with uneven size and shape to be easily modified into monodisperse nanospheres with ultrasmall sizes of ∼5 nm in a solution system. The possible mechanism is as follows: Each substitution of Sr^{2+} by Ln^{3+} in SrF_2 requires an extra F^- for charge compensation, and the introduction of such F^- ions into the grain surface may induce transient electric dipoles with their negative poles outward. These transient electric dipoles hinder the diffusion of F^- ions (which are needed for crystal growth) from the solution to the grain surface, thus retarding the growth of SrF_2. It is further proved that this strategy is versatile for the controllable synthesis of monodisperse alkaline-earth fluorides (MF_2) with ultrasmall size. Evidently, the Ln^{3+}-doped MF_2 nanocrystals exhibit bifunctionality, i.e., tunable upconversion (UC) luminescence and proper paramagnetism, and therefore may find potential applications in the biological field.

The selection of alkaline-earth fluorides as the doping host was motivated by their high solubility for trivalent lanthanide ions substituting for divalent alkaline earth ions as well as their low phonon energy, which favors suppression of nonradiative losses and thereby improves the luminescence of the optically active dopants.[9] The lanthanide-doped SrF_2 nanocrystals were prepared by the modified liquid−solid solution (LSS) solvothermal route reported by Li and co-workers[10] (see the Experimental Section in the Supporting Information). Transmission electron microscopy (TEM) observations (Figure 1a) showed that the pure SrF_2 nanocrystals had a bimodal distribution, i.e., some irregular particles were big, while others were much smaller with multiplex shapes such as nanospheres, nanocubes, and nanoplates. However, after lanthanide doping, the size (and its distribution) and shape of the SrF_2 nanocrystals were remarkably modified. As shown in Figure 1b, the monodisperse La^{3+}-doped SrF_2 nanocrystals were spherically shaped with a uniform diameter of ∼5 nm (upper inset of Figure 1b). The single-crystalline nature of these nanoparticles was revealed by high-resolution TEM (HRTEM) (Figure S1 in the Supporting Information), and the incorporation of La^{3+} ions into the SrF_2 nanocrystals was verified by energy-dispersive X-ray spectroscopy (EDS) (bottom inset of Figure 1b). As shown in Figure S2, the X-ray diffraction (XRD) patterns of the samples match well with that of standard cubic SrF_2 (JCPDS 06-0262). Obviously, the XRD pattern of the pure SrF_2 basically consists of two sets of diffraction peaks: one is sharp and ascribed to big grains while the other is broad and corresponds to small ones, verifying the bimodal distribution of SrF_2 particles. In contrast, the XRD pattern of the La^{3+}-doped sample exhibits only one set of broad peaks, indicating the uniform small grain size, in agreement with the TEM observations.

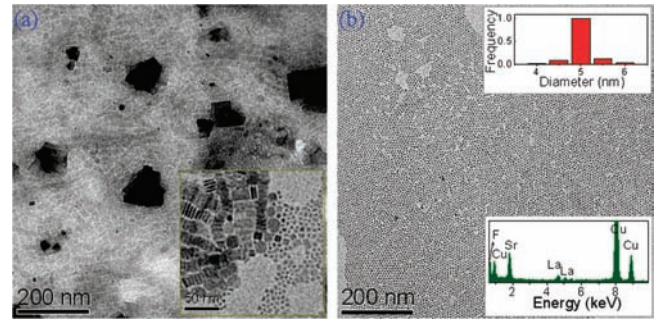

Figure 1. (a) TEM micrograph of pure SrF_2 nanocrystals. The inset shows an enlarged image of small nanocrystals with multiplex shapes. (b) TEM micrograph of 20 mol % La^{3+}-doped SrF_2 nanospheres. The upper inset shows a histogram of the particle size distribution and the lower one the EDS spectrum taken from the nanospheres (Cu signals come from the copper grid).

To elucidate the mechanism of modifying the SrF_2 crystal growth by lanthanide doping, SrF_2 nanocrystals doped with other impurities (20 mol % Gd^{3+}, Yb^{3+}, Ca^{2+}, or Ba^{2+}) were also prepared. As exhibited by Figures S3−S6, Gd^{3+} and Yb^{3+} doping showed effects similar to those of La^{3+} doping on the growth of SrF_2 nanocrystals, while Ca^{2+} or Ba^{2+} doping had no obvious impact. The evolution of the XRD peaks for SrF_2 nanocrystals doped with various contents of Yb^{3+} are presented in Figure S7. Remarkably, the intensity of the sharp peaks, i.e., the number of big SrF_2 crystals, decreased with increasing Yb^{3+} doping content, and these peaks disappeared

10.1021/ja1036429

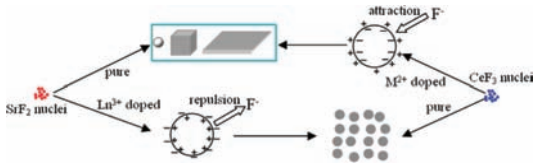

Figure 2. Schematic illustration of the modifications of impurity doping on the size and shape of SrF_2 and CeF_3 nanocrystals.

completely when the Yb^{3+} content reached 10 mol %. TEM observations (Figure S8) provided evidence that the size of those small nanocrystals was gradually reduced and the size distribution tended to be more homogeneous with increasing Yb^{3+} content. Notably, to ensure the formation of monodisperse SrF_2 nanocrystals in the pure phase, the highest Ln^{3+} doping content was found to be ~40 mol % under the current synthesis conditions. The variation of the SrF_2 lattice induced by Ln^{3+} doping is discussed in the Supporting Information.

The possible modification mechanism of lanthanide doping on the size and shape of the SrF_2 nanocrystals is schematically illustrated in Figure 2. In the LSS solvothermal system, the oleic acid-capped Sr^{2+} ions at first react with F^- ions to form oleic acid-capped SrF_2 crystalline nuclei. When the reaction is prolonged, the SrF_2 nuclei quickly grow, benefitting from F^- diffusion from the aqueous solution to the nanocrystals, similar to the situation reported for the growth of $NaYF_4$.[8] After Ln^{3+} ions are added into the system, they occupy Sr^{2+} sites. In order to establish charge balance, for each doped Ln^{3+} ion, an extra F^- ion is introduced into the grain surface coupling with this Ln^{3+} ion.[9a,b] In this case, transient electric dipoles with the negative poles pointing outward may be formed on the nanocrystal surface, which substantially slows the diffusion of the F^- ions needed for crystal growth from the solution to the crystal as a result of the charge repulsion, consequently resulting in retardation of the SrF_2 nanocrystal growth.

To demonstrate the versatility of the proposed mechanism, we extended the experimental study to other related systems. With the same method, pure as well as 20 mol % La^{3+}-doped CaF_2 and BaF_2 nanocrytals were prepared and characterized. Definitely, the growth of CaF_2 and BaF_2 nanocrystals was also modified by lanthanide doping, similar to the case for SrF_2, as evidenced by Figures S9 and S10. Moreover, the impact of alkaline-earth (M^{2+}) ion doping on the growth of CeF_3 and LaF_3 nanocrystals under the analogous solution conditions was also studied to further validate the mechanism from the reverse angle (see Figures S11 and S12). As expected, upon addition of Ca^{2+} or Sr^{2+}, monodisperse spherical CeF_3 and LaF_3 nanocrystals grew, and their shapes tended to be multiplex. At a moment when M^{2+} ions take up Ce^{3+} or La^{3+} sites in the lattice, positive vacancies are generated on the grain surface to balance the charge, forming transient electric dipoles with the positive poles pointing outward that greatly accelerate the diffusion of F^- ions from the solution to the grain and therefore promote the growth of CeF_3 and LaF_3 nanocrystals (see Figure 2).

Under 975 nm excitation, these MF_2 nanocrystals doped with specific lanthanide ions exhibit bright UC luminescence. As shown in Figure 3a,b, the $Gd^{3+}/Yb^{3+}/Er^{3+}$ triply doped SrF_2 nanocrystals in cyclohexane emit dominant green as well as weak blue and red UC light ascribed to Er^{3+} $4f^{11} \rightarrow 4f^{11}$ transitions, whereas the $Gd^{3+}/Yb^{3+}/Tm^{3+}$ triply doped ones yield intense blue as well as weak red and near-IR light resulting from the Tm^{3+} $4f^{12} \rightarrow 4f^{12}$ transitions (the UC mechanisms are illustrated in Figure S13). With the same method used by Chen and co-workers[11] (see the Supporting Information), the green and blue UC efficiencies were roughly estimated to be ~1.2 and ~0.5%, respectively. The inset of Figure 3 displays photographs of the eye-visible green and blue UC luminescence. Apart from the excellent UC luminescence, these triply doped SrF_2 nanocrystals also exhibit paramagnetism at room temperature (Figure 3c) that originates from the intrinsic magnetic moment of Gd^{3+} ions a with noninteracting and localized nature.[12] The magnetization of the nanocrystals at 20 kOe is ~1.4 emu/g, which is close to the value reported for nanoparticles used for common bioseparation.[13]

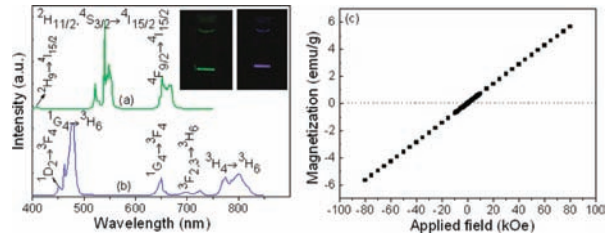

Figure 3. Upconversion emission spectra of SrF_2 nanocrystals triply doped with (a) 10 mol % Gd^{3+}/10 mol % Yb^{3+}/1 mol % Er^{3+} and (b) 10 mol % Gd^{3+}/10 mol % Yb^{3+}/1 mol % Tm^{3+} under near-IR laser excitation. The insets show photographs of the corresponding eye-visible upconversion luminescence. (c) Magnetization as a function of applied field for 10 mol % Gd^{3+}/10 mol % Yb^{3+}/1 mol % Er^{3+} triply doped SrF_2 nanocrystals.

Lemieux−von Rudloff reagent was used to oxidize the oleic acid ligands on the surfaces of the UC SrF_2 nanocrystals to azelaic acids, similar to the case for $NaYF_4$.[14] These oxidized nanoparticles were nearly monodisperse and could be well-dispersed in water, with their UC emission intensity equivalent basically to that of the original hydrophobic ones (Figure S14). Hopefully, these ultrasmall bifunctional nanoparticles may find potential applications in fluorescent bioprobes and magnetic resonance imaging.

In summary, this study has offered a simple route for modifying the uneven size and shape of the alkaline-earth fluoride nanophases to monodisperse ultrasmall nanospheres through lanthanide doping. These nanospheres exhibit bifunctionality, i.e., tunable upconversion emissions as well as proper paramaganetism, making them potentially applicable in the biological field. The synthesis strategy, which involves doping of an impurity with a different valence than the cation in the nanophase, might be useful for controlling the solution growth of some technologically important nanomaterials.

Acknowledgment. We thank Prof. X. Y. Chen and Dr. Y. S. Liu for providing UC $NaYF_4$ samples and for helpful discussions of luminescence efficiency measurements. This work was supported by the National Natural Science Foundation of China (10974201 and 50902130).

Supporting Information Available: Experimental details, Table S1, and Figures S1−S14. This material is available free of charge via the Internet at http://pubs.acs.org.

References

(1) (a) Zhang, F.; Braun, G. B.; Shi, Y.; Zhang, Y.; Sun, X.; Reich, N. O.; Zhao, D.; Stucky, G. *J. Am. Chem. Soc.* **2010**, *132*, 2850. (b) Abel, K. A.; Boyer, J. C.; van Veggel, F. C. J. M. *J. Am. Chem. Soc.* **2010**, *131*, 14644. (c) Mahalingam, V.; Bovero, E.; Munusamy, P.; van Veggel, F. C. J. M.; Wang, R.; Steckl, A. J. *J. Mater. Chem.* **2009**, *19*, 3889. (d) Sangeetha, N.; van Veggel, F. C. J. M. *J. Phys. Chem. C* **2009**, *113*, 14702.

(2) (a) Mahalingam, V.; Vetrone, F.; Naccache, R.; Speghini, A.; Capobianco, J. A. *Adv. Mater.* **2009**, *21*, 4025. (b) Vetrone, F.; Mahalingam, V.; Capobianco, J. A. *Chem. Mater.* **2009**, *21*, 1847. (c) Vetrone, F.; Naccache, R.; Mahalingam, V.; Morgan, C. G.; Capobianco, J. A. *Adv. Funct. Mater.* **2009**, *19*, 2924.

(3) (a) Wang, F.; Liu, X. G. *Chem. Soc. Rev.* **2009**, *38*, 976. (b) Jiang, C. L.; Wang, F.; Wu, N. Q.; Liu, X. G. *Adv. Mater.* **2008**, *20*, 4826. (c) Wang, F.; Liu, X. G. *J. Am. Chem. Soc.* **2008**, *130*, 5642.

(4) (a) Du, Y. P.; Zhang, Y. W.; Yan, Z. G.; Sun, L. D.; Yan, C. H. *J. Am. Chem. Soc.* **2009**, *131*, 16364. (b) Li, Y. P.; Zhang, J. H.; Zhang, X.; Luo, Y. S.; Lu, S. Z.; Ren, X. G.; Wang, X. J.; Sun, L. D.; Yan, C. H. *Chem.*

Mater. **2009**, *21*, 468. (c) Jia, C. J.; Sun, L. D.; Luo, F.; Jiang, X. C.; Wei, L. H.; Yan, C. H. *Appl. Phys. Lett.* **2004**, *84*, 5305.

(5) (a) Zhang, H.; Li, Y.; Ivanov, I.; Qu, Y.; Huang, Y.; Duan, X. *Angew. Chem., Int. Ed.* **2010**, *49*, 1. (b) Lim, S.; Ryu, W.; Austin, R. *Opt. Express* **2010**, *18*, 2309. (c) Luwang, M. N.; Ningthoujam, R. S.; Jagannath; Srivastava, S. K.; Vatsa, R. K. *J. Am. Chem. Soc.* **2010**, *132*, 2759.

(6) Norris, D.; Efros, A.; Erwin, S. *Science* **2008**, *319*, 1776.

(7) Feng, X.; Sayle, D.; Wang, Z.; Paras, M.; Santor, B.; Sutorik, A.; Sayle, T.; Yang, Y.; Ding, Y.; Wang, X.; Her, Y. *Science* **2006**, *312*, 1504.

(8) Wang, F.; Han, Y.; Lim, C.; Lu, Y.; Wang, J.; Xu, J.; Chen, H.; Zhang, C.; Hong, M.; Liu, X. *Nature* **2010**, *463*, 1061.

(9) (a) Franklin, A. D. *J. Chem. Phys.* **1976**, *64*, 1509. (b) Sobolev, B.; Seiranian, K.; Garashina, L.; Fedorov, P. *J. Solid State Chem.* **1979**, *28*, 51. (c) Zhang, X.; Quan, Z.; Yang, J.; Yang, P.; Lian, H.; Lin, J. *Nanotechnology* **2008**, *19*, 075603. (d) Zhang, C.; Li, C.; Peng, C.; Chai, R.; Huang, S.; Yang, D.; Cheng, Z.; Lin, J. *Chem.—Eur. J.* **2010**, *16*, 5672. (e) Quan, Z.; Yang, D.; Yang, P.; Zhang, X.; Lian, H.; Liu, X.; Lin, J. *Inorg. Chem.* **2008**, *47*, 9509. (f) Zhang, C.; Hou, Z.; Chai, R.; Cheng, Z.; Xu, Z.; Li, C.; Huang, L.; Lin, J. *J. Phys. Chem. C* **2010**, *114*, 6928. (g) Wang, Z.; Quan, Z.; Jia, P.; Lin, C.; Luo, Y.; Chen, Y.; Fang, J.; Zhou, W.; O'Connor, C. J.; Lin, J.*Chem. Mater*. **2006**, *18*, 2030.

(10) (a) Wang, X.; Zhuang, J.; Peng, Q.; Li, Y. D. *Nature* **2005**, *437*, 121. (b) Zhuang, Z.; Peng, Q.; Zhang, B.; Li, Y. D. *J. Am. Chem. Soc.* **2008**, *130*, 10482. (c) Wang, G.; Peng, Q.; Li, Y. D. *J. Am. Chem. Soc.* **2009**, *131*, 14200. (d) Xie, T.; Li, S.; Peng, Q.; Li, Y. D. *Angew. Chem., Int. Ed.* **2009**, *48*, 196. (e) Li, S.; Xie, T.; Peng, Q.; Li, Y. D. *Chem.—Eur. J.* **2009**, *15*, 2512.

(11) Liu, Y.; Tu, D.; Zhu, H.; Li, R.; Luo, W.; Chen, X. *Adv. Mater*. [Online early access]. DOI: 10.1002/adma.201000128. Published Online: June 8, 2010.

(12) Wong, H.; Chan, H.; Hao, J. *Appl. Phys. Lett.* **2009**, *95*, 022512.

(13) (a) Dosev, D.; Nichkova, M.; Dumas, R. K.; Gee, S. J.; Hammock, B. D.; Liu, K.; Kennedy, I. M. *Nanotechnology* **2007**, *18*, 055102. (b) Liu, Z.; Yi., G.; Zhang, H.; Ding, J.; Zhang, Y.; Xue, J. *Chem. Commun.* **2008**, 694.

(14) Chen, Z.; Chen, H.; Hu, H.; Yu, M.; Li, F.; Zhang, Q.; Zhou, Z.; Yi, T.; Huang, C. *J. Am. Chem. Soc.* **2008**, *130*, 3023.

JA1036429